Remotely controlled observations of electro-optical upper atmospheric phenomena from Baja, Hungary

József Bór[1*], Tibor Hegedüs[2], Zoltán Jäger[2], Tibor Molnár[1], Csaba Molnár[1], Csongor Szabó[1], Karolina Szabóné André[1], Zoltán Zelkó[2] and László Döbrentei[3]

[1]Institute of Earth Physics and Space Science (ELKH EPSS), Sopron, Hungary

[2]Baja Observatory of the University of Szeged, Baja, Hungary

[3]Research Centre for Astronomy and Earth Sciences (ELKH CSFK), Budapest, Hungary

Abstract

A remotely manageable optical observation system for recording transient luminous events (TLEs) in the upper atmosphere was installed in Baja, Hungary in 2014. This report describes hardware components and settings of the system, software solutions applied either for realtime event detection and remote control, and the strategy of actually making the observations. An overview on the number and type of TLEs observed up to 2020 is presented. During the 7 years of operation, 1655 TLEs were recorded, 92.7% of which were red sprites, 6.4% were sprite halos, and the set of captured events contained altogether only 3 ELVES. Most sprites were observed in June while most sprite halos were observed in September over the years covered in this report.

Keywords: transient luminous events, optical observations, remote control solution.

Introduction

The existence of sub-ionospheric optical emissions of various peculiar forms and characteristic dynamics with durations less than a second were proved mostly in the late 80's and 90's. These phenomena are optically observable signatures of electrical excitation processes which take place in the atmosphere above the clouds of electrically active thunderstorms. As the parent processes that trigger the appearances of these phenomena are directly linked to fast charge transport in the thundercloud (i.e., intense charge separation and lightning strokes), we refer to these events as electro-optical upper atmospheric phenomena or transient luminous events (TLEs).

*Corresponding author: József Bór (bor.jozsef@epss.hu)

Citation: Bór, J., Hegedüs, T., Jäger, Z., Molnár, T., Molnár, Cs., Szabó, Cs., Szabóné André, K., Zelkó, Z., and Döbrentei, L. (2021): Remotely controlled observations of electro-optical upper atmospheric phenomena from Baja, Hungary. *Geophysical Observatory Reports 2020*, 51-65. https://doi.org/10.55855/gor2020.7

Present knowledge on physical processes behind the initiation and development of the various emission types, i.e., ELVES, red sprites, sprite halos, blue starters, blue jets, gigantic jets and upward lightning discharges is summarized in comprehensive review papers (Pasko et al., 2012; Siingh et al., 2012; Surkov & Hayakawa, 2020).

TLEs provide an alternative way to study extreme lightning activity in thunderstorms and chemical as well as physical interactions including electrodynamic coupling processes in the upper atmosphere (Siingh et al., 2011; Gordillo-Vázquez & Péter-Invernón, 2021). This explains why efforts are made worldwide to register the occurrences of these events using both ground-based recording facilities and space-borne observations (Hsu et al., 2017; Neubert et al., 2019; Arnone et al., 2020).

Organized observations of TLEs from Hungary started in 2007 in Sopron to serve scientific research (Bór et al., 2009; Bór, 2013; Bór et al., 2018). The site provides fairly good observational coverage in middle Europe over Hungary, Slovakia, the Czech Republic, Austria, south-east Germany, south Poland, Slovenia, Croatia, the northern part of Serbia and Bosnia, and the western part of Romania (Bór et al., 2009). Especially during autumn and winter, however, lightning activity is more pronounced over the Mediterranean region (Arnone et al., 2020). To cover more area to the south of Hungary in these time periods, a second observation system was set up in the south part of the county in Baja in 2014 (Fig. 1). In this report, we briefly describe the hardware and software components of the system as well as the methodology which is applied in the observations. Then, observations made since the installation of the system up to the year 2020 are summarized.

The site: Astronomical Observatory in Baja

The observatory (46.180278° N, 19.010833° E, 110 m above mean sea level) is about 4 km away from the city center of Baja, close to the southern border of Hungary. The corresponding area is about 4 ha large. It is a protected area and the light pollution is low. The building of the observatory was constructed in 1981 and the astronomical research staff moved here from the city centre in 1986. From this time on, the original scope of research in Baja that addresses studying the upper atmosphere on the base of satellite observations (Ill, 1983) has been extended to include classic stellar astronomy. The only telescope in the observatory between 1985 and 1992 was a 40 cm Cassegrainian reflector (property of the University of Szeged) and photometric observations of selected eclipsing binaries were made almost each clear night (Hegedűs et al., 1992). Following a period of uncertainties in financing, a new main telescope (50 cm f/8.4 RC) was installed in Baja in 1995. The development of a large-field telescope (50 cm refractor, f/6) started in 2005. This instrument has become the first Hungarian robotic photometric telescope with an SDSS filter system. Based on this telescope, a new observation program, the BASSUS supernovae program (Vinkó et al., 2012) has been initiated by the University of Szeged. This has led to setting up a new 80 cm f/7 RC robotic telescope in 2020 in the observatory. Presently, the main activity in the observatory is related to supernovae research as well as observations of eclipsing binaries and multiple star

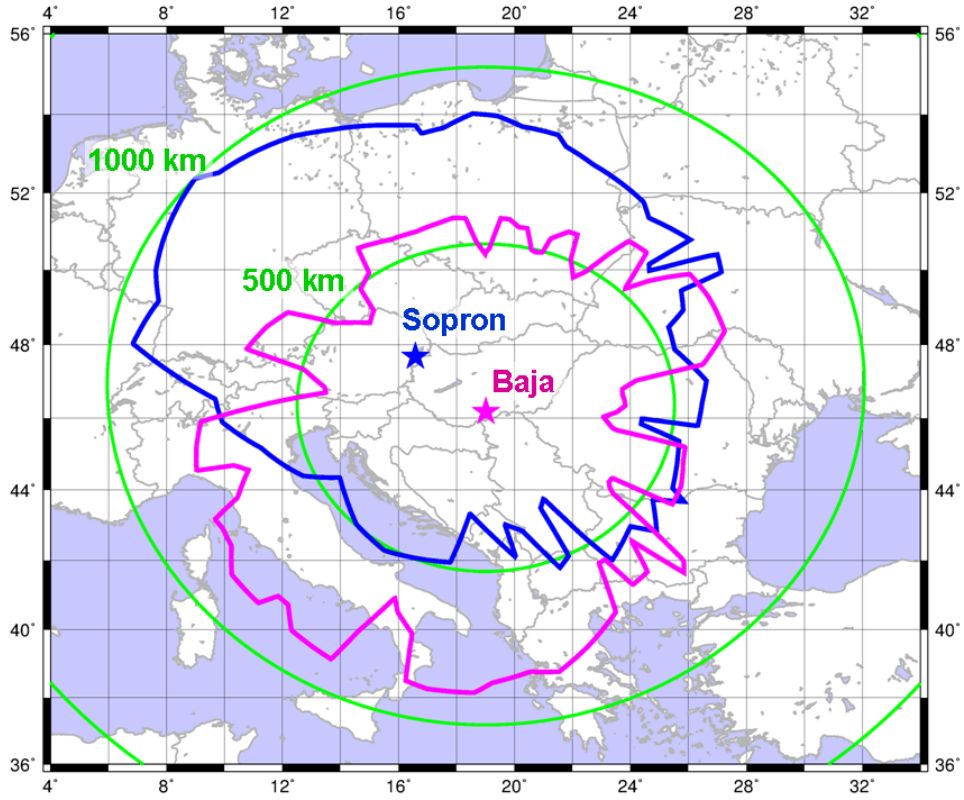

Fig. 1: Observational coverage for watching above 50 km altitude from Baja and from Sopron.

systems (Mitnyan et al., 2018). Beyond these main directions of astrophysical research, the area of scientific activities in Baja includes more multidisciplinary fields of studies like meteor science or near-Earth space phenomena. TLE observations fit well into these new lines. Figure 2 shows the building of the observatory with the camera mounted on the roof.

Components of the optical observation system

Hardware components of the optical part of the observation system in Baja are similar to those that have been used in Sopron (Bór et al., 2009), but there are minor differences. The camera is of the same type as that in Sopron, i.e., a Watec 902H2 Ultimate (1/2", CCIR). On the camera, uniform backlight area is set (the default state), electronic shutter is switched off and the auto exposure (AE) mode is set to position 8 where the exposure index (EI) is off and the lowest shutter speed is 1/50 s. Gamma is set to LO ($\gamma \approx 0.45$). Manual gain control mode is selected

Fig. 2: Baja Astronomical Observatory with the TLE camera on the roof (zoomed-in image is on the inset).

and the gain is set to have the noise level and the brightness of the acquired picture balanced. This way, relatively faint events can be detected without having too many false detections due to large noise fluctuations.

The camera is equipped with a Tamron 12VG412ASIR aspherical, IR corrected lens in Baja. The maximum f-stop value of this lens is 1.2. The focal length of the lens was set so that the effective size of the field of view (48° horizontally, 35° vertically) is similar to that in Sopron. Experience shows that this setup provides a fairly wide viewing angle and, at the same time, fairly detailed images of TLEs. Analog video signals are channeled through a video time inserter (TIM-10) to have a time stamp on each video frame so that the start and end of the exposure time of each video half frame (covering 20 ms) can be read directly with millisecond accuracy. The signals are digitized in the recording computer by a Leadtek WinFast VC100XP PCI digitizer card in a standard resolution of 720x576 pixels.

During observation, consecutive digitized video frames are evaluated realtime by the UFO Capture event detection software (version 2.22). The software is set to trigger on the simultaneous brightening of 15 pixels or more. To detect brightening reliably and still be able to capture faint events, noise tracking is enabled in the software and the ratio of the detection level to the noise level is set only to 105% with a minimum difference of 2 units required between them. It was found that the gain on the camera is close to optimal when the detect level is at around 40-45 units during normal monitoring without any event occurring. The corresponding gain

setting was found by experience. To reduce the number of false detections due to cosmic ray events that brighten up only a few pixels in just one frame, the minimum duration for an event to raise a normal trigger (parameter 'Min(frm)') was set to 2 frames. At the same time, the minimum number of brightened pixels that maintain this state (detect size) was set to 2 to record even very small events of relatively longer duration. Additionally, irrelevant parts of the actual view (e.g., buildings, trees, and the overlaid time stamp) as well as failing pixels of the camera CCD were masked out. The dark object mask feature was enabled at level 2, identification of slow objects (e.g. airplanes) was turned on (highest speed 15, size 15), and the scintillation mask option was switched on (level 105, speed 2, size 5). This latter setting allows the software to detect and register stars, which are the most common scintillating objects in the night sky. A utility software was developed to distinguish static scintillating pixels (usually due to CCD degradation) from stars, the position of which changes on the image with time. Note that the position of the camera should not change in the evaluation period. Other scintillating pixels are masked and the stars can then be used to determine the actual direction of the camera and the events within the field of view very accurately. Once a trigger had been raised, a short clip of the event was recorded with 10 frames both before and after the triggering video frame.

Remote controlling of the observations

The optical system can cover only a limited part of the sky at a time. Areal coverage can be extended by using a pan-tilt solution to aim the camera above actually active thunderstorms occurring in any direction and distance within the observable distance range. A unique, weather resistant, remotely controllable camera-directing solution was developed and installed in Baja for the first time. The system is based on a Videotec PTH-355P pan-tilt unit (PTU) with which the camera can be moved by DC motors and the actual pan and tilt positions can be determined from analog signal outputs. A controlling electronics was developed to serve as an interface between the PTU and the computer that runs the detection software. It provides the user with the possibility of changing the position of the camera as needed. The system can set the azimuth and elevation angle of the camera with an accuracy of 0.1°. The electronics allows the user to switch on or off heating in the camera house to lower the relative humidity in the camera house. Additionally, controlling the electronic iris on the lens can be taken over from the camera and the iris can be set to stay fully open or closed. While automatic iris control can save the CCD from being exposed to very strong light directly for a long time, this feature of the controlling electronics is very useful in cases when the reaction time of the automatic iris control is slow or when disturbing lights in an irrelevant part of the picture would otherwise cause the iris to close so that fainter events would be missed. Note that only a 338° wide azimuth range can be set on the PTU. In spite of that, the full 360° azimuth range is covered because the wide field of views of the camera overlap at the two end-azimuth positions. All functions of the PTU-controlling electronics can be accessed through serial connection using a simple RS232 terminal program.

The data acquisition PC, the camera, and other hardware parts of the system don't need to be switched on all the time. To allow switching on and off these devices as needed, a power switch was developed which can be controlled remotely and independently from other units in the detection system through a web interface. The power switch is based on a SR-201 2-way Ethernet relay board, the capability of which has been extended so that it can manage the powered state of 8 different devices.

A PC is used to control all units in the detection system. This control includes setting up and running the event detection software, directing the camera, heating of the camera house, and setting the state of the iris. Note that the power switch can be controlled independently from the PC. Video clips and observation logs are collected locally and some of the pre-processing tasks are also carried out on that computer. These complex tasks require the observer to have full control over the PC. Application of the Tiger VNC software was found to be a bandwidth-friendly solution that is proved to serve this need reliably. To save the camera from strong daylight, an algorithm was created and implemented in PHP coding language to shut down both software and hardware components of the observations system properly and automatically. The code is scheduled to run around surface sunrise times at Baja.

Methodology of the observations

TLEs can be detected during the night in low-light conditions when scattered sunlight doesn't mask the relatively small number of photons emitted during these events. TLEs appear above thunderstorms in which charge separation processes are very active (Pasko et al., 2012). Therefore, it must be determined whether there are active nighttime thunderstorms anywhere within the area above which the height range of typical TLE occurrences (e.g., 50-90 km for red sprites) can be fully observed from the recording site. This range is determined from images on which the horizon around the site is visible. After the direction of the camera is determined by matching the stars in the image to the sky map at the time point when the image was taken, the elevation of points right above the horizon is determined at several azimuths. Finding these elevations can be accomplished by using the UFO Analyzer program. Then, the maximum distance within which one can see the atmosphere only above any given altitude can be calculated (Fig. 3). Note that the curvature of the Earth must be taken into account. These distances depending on the azimuth border the covered area around the site (Fig. 1).

Occurrence of active thunderstorms can be forecasted. A forecast can be found on the webpage of the European Storm Forecast Experiment project (ESTOFEX, 2021). Actual presence of active thunderstorms within the covered area can be checked on realtime lightning maps which are produced by a number of services and can be found at several websites (left panel on Fig. 4). Some examples are BlitzOrtung (2021); LightningMaps (2021); Meteologix (2021).

Satellite images showing infrared (IR) cloud top temperatures are another useful source of information (AllMetSat, 2021). On one hand, the development and time

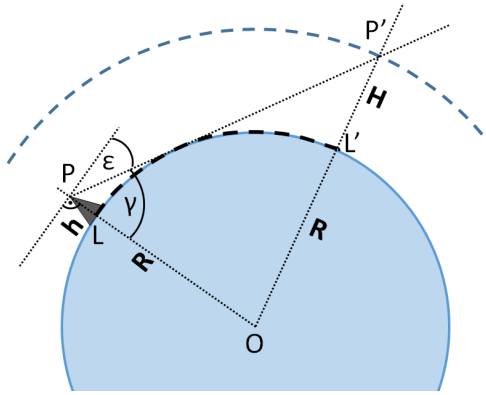

Fig. 3: Geometry for determining the range LL' from the point of observation P at a height h above main sea level within which one can see the atmosphere above the altitude H above main sea level. The radius of the earth is R and ϵ is the elevation angle of the horizon in P. First, γ must be calculated and then the POP'Δ needs to be solved for the LOL' angle using the law of cosines.

evolution of the active thunderstorm cells can be followed by monitoring the series of IR images. Active cells feature intense updraft in which moist air is lifted towards the upper troposphere where it cools down and clouds form. This process can be seen in the images as rapidly appearing and extending, rather localized white spots of very cold cloud tops (Schmetz et al., 1997) (right panel on Fig. 4). On the other hand, IR images can give a hint whether there are any clouds between the observation site and the region of interest. Such clouds may block the view and can make successful observations impossible. Note that the clouds move and transform fairly quickly and the cloud cover is not necessarily continuous, so it in fact happened that TLEs were recorded between clouds or through discontinuities of the cloud cover. In any case, local viewing conditions must be good. In Baja, this can also be checked using all-sky images from an independent camera which is installed locally. The number of stars visible closely above the horizon indicates well the presence of long-distance visibility. The more stars can be seen, the better the viewing conditions are.

Red sprites are a type of TLEs which are most often recorded by common optical systems in ground-based observations (Arnone et al., 2020). Therefore, the camera is usually set to capture these events with high probability. The appearance of sprites is triggered by intense positive cloud-to-ground (+CG) lightning strokes (van der Velde et al., 2014). Sprite events are known to appear at various distances behind the convective cores above the stratiform region of the thundercloud in the mature state of the thunderstorm (Soula et al., 2015; Bór et al., 2018; Wang et al., 2019). While the location of thundercloud cells of deep convection can be estimated

and the extension of the stratiform cloud region can be guessed from satellite IR images, the most reliable sources of this information are weather radar composite images. One service where radar images can be found is the radar animation service from Eumetnet (Saltikoff et al., 2019)[†].

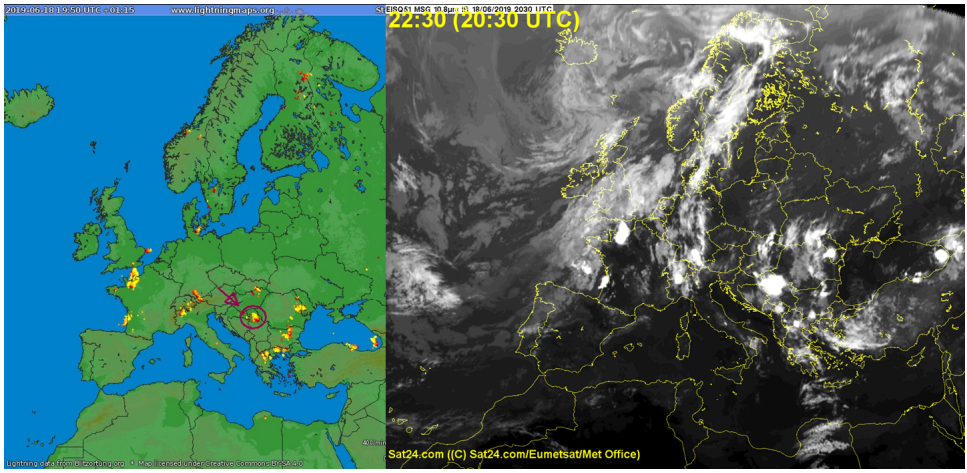

Fig. 4: Resources for determining the location of active thunderstorms. **Left:** Lightning map from BlitzOrtung/Lightningmaps.org. The storm cell which produced TLEs that were recorded in Baja is marked. **Right:** a corresponding Meteosat IR cloud top temperature image.

In practice, the observer first checks if there are any potentially TLE-producer thunderstorms within the observable area. If there is at least one storm of such and the local viewing conditions are good, the camera is turned on and will be directed toward the most promising storm so that both the active cells and the corresponding stratiform region of the storm to be within the horizontal viewing angle. The elevation angle of the camera must be chosen so that as thick height region below the altitude of 100 km to be covered as possible (Fig. 5).

If an observer is available to make observations on a night, the following information is logged: presence or absence of potentially TLE-active thunderstorms within the covered area, any circumstance that may interfere with successful observations (e.g., intervening clouds, poor local visibility, system malfunction, etc.). If any observations are made, the camera positions and system commands (e.g. switching on and off the camera, or iris control) are logged by the directing system. In addition to the video clip of each recorded event, the UFO Capture software saves the actual scintillation map and brightness peak-hold image of the video clip along with an

[†]https://www.eumetnet.eu/activities/observations-programme/current-activities/opera-radar-animation/

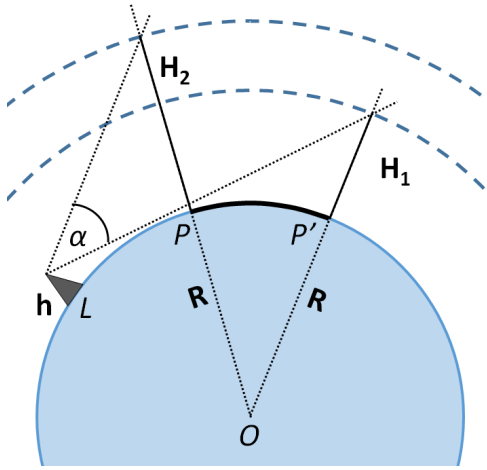

Fig. 5: A limited distance range PP' from the observer in location L is covered fully by a camera of a given vertical viewing angle α if an altitude range between heights H2 and H1 is to be monitored.

XML file containing the parameters with which the program was operated.

During initial post-processing, the events are reviewed one by one to identify TLEs. Then, the appearance time of the event is extracted from the time stamps in the video clip and the type of the TLE (red sprite, sprite halo, ELVES, etc.) is identified by visual inspection. Finally, the area of TLE production is determined roughly for distinct periods of TLE production which are clearly separated from one another by longer pauses (about 30-40 minutes) in the occurrences of events. Bordering coordinates of the production area are read in a resolution of 0.5° or 1° (depending on the ambiguity of the case) from lightning maps on which cumulated lightning activity in the TLE production period is displayed.

Overview of the observations from 2014 to 2020

During the first 7 years of operation, altogether 1655 different TLEs were recorded by the camera in Baja. The vast majority of the events were red sprites (1535), but sprite halos also were detected (106). Only 3 ELVES were recorded and the set includes 4 more events the type of which could not be identified unambiguously. The left panel in Fig. 6 shows the number of recorded events in each year. Note that these events were recorded on different numbers of nights in those years, so the average number of observed events on a night gives a somewhat better impression on the general intensity of sprite production in a year. This is shown on the right panel in Fig. 6. Note that the standard deviations are almost always greater than the mean value which indicates that the corresponding distribution is not normal.

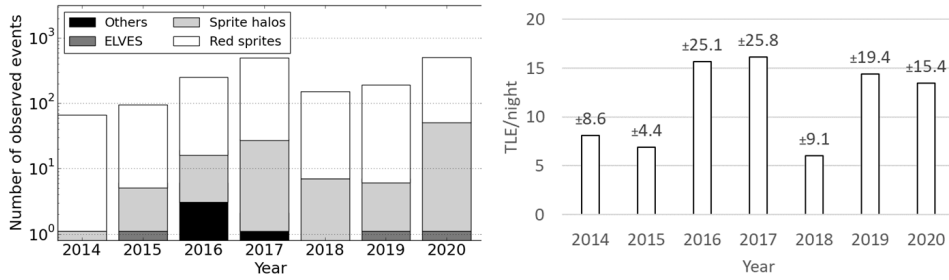

Fig. 6: Yearly summary of TLE records from Baja in the period 2014-2020. **Left:** number and types of observed events. Note the logarithmic scale. **Right:** average number of TLEs recorded in different years. The number of nights of successful observations was 9 in 2014, 13 in 2015, 15 in 2016, 29 in 2017, 24 in 2018, 13 in 2019, 34 in 2020. The standard deviations are written above each column.

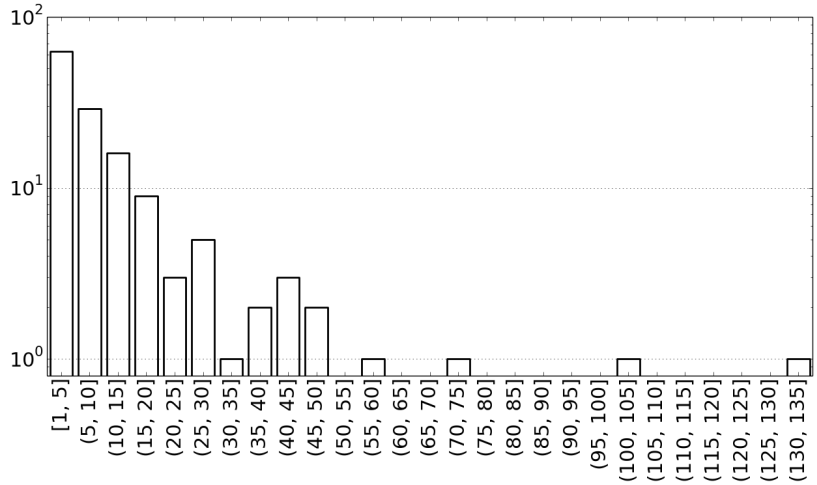

Fig. 7: Distribution of the number of TLEs that were observed on a single night from Baja in the period 2014-2020. Note the logarithmic scale.

Indeed, these statistics can be biased by exceptionally TLE-active thunderstorms which can produce an outstanding number of events on a single night. The distribution of events observed on a night (Fig. 7) clearly indicates this. In the considered years, the number of events observed on a single night was above 100 two times: 102 events were recorded on Sept 5, 2016, and 132 events were recorded on Aug 10, 2017. The histogram shown in Fig. 7 well mirrors the power law found for the number of events produced by lightning activity in a single thunderstorm in Europe (Arnone et al., 2020).

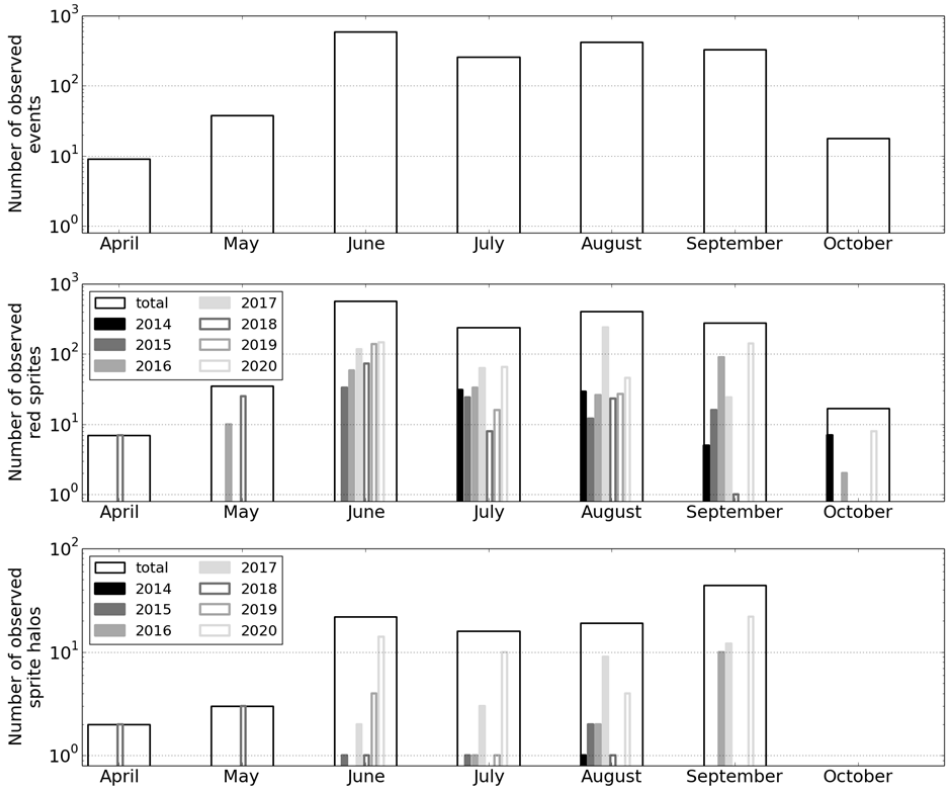

Fig. 8: Monthly number of TLEs observed from Baja in the period 2014-2020. **Upper panel:** total number of events. **Middle panel:** red sprites. **Lower panel:** sprite halos.

Observations were made in months from June to September almost in each year between 2014 and 2020, so comparing the number of observed TLEs in these months is meaningful (Fig 8). It can be seen that the most TLEs were observed in June and sprite occurrences dominate in this month. The outstanding number in August is only due to the exceptionally high number of events that were observed in 2017.

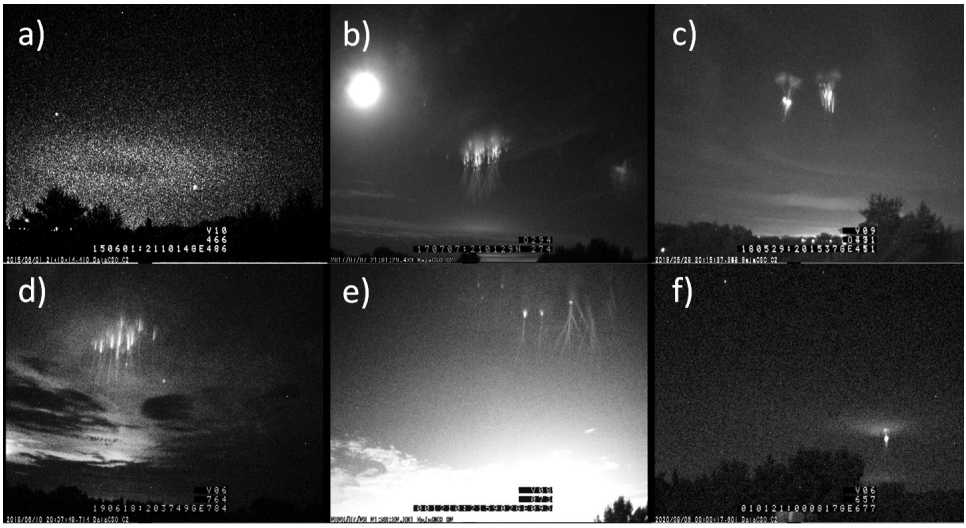

Fig. 9: Examples of TLEs observed from Baja. **a)** ELVES, Jun 1, 2015, 21:10 UTC, **b)** sprite cluster and the Moon, Jul 7, 2017, 21:01 UTC, **c)** carrot sprites, May 29, 2018, 20:15 UTC, **d)** sprite cluster close to Baja, Jun 18, 2019, 20:37 UTC, also see Fig. 4, **e)** very short column sprites with bright tendrils, Jul 26, 2020, 21:59 UTC, note the week number rollover error in the time stamp **f)** carrot sprite and sprite halo, Sep 6, 2020, 00:08 UTC, note the week number rollover error in the time stamp.

The middle and lower panels in Fig. 8 also reveal that the number of observed sprite halos does not have an obvious peak in any month of the observation period. Again, the outstanding number in September appears because of the great number of events detected in 2020. This difference between the observed numbers of these TLE types suggests that there may be a change in the characteristics of lightning strokes as autumn follows summer (Rakov & Uman, 2007, ch. 2.8, ch. 8), and the center of the lightning activity tends to move to the south (Arnone et al., 2020; Kotroni & Lagouvardos, 2016). Figure 9 shows examples of TLEs recorded in the considered years.

Summary

The second observation site in Hungary in support of organized scientific research on TLEs has been set up in the Astronomical Observatory in Baja in 2014. Since the installation up to 2020, 1655 TLEs were recorded above the covered area in Europe. The vast majority of the captured events are sprites but several sprite halos (106) were captured, too. Only 3 ELVES were detected unambiguously. Both the total number of recorded events and the average number of events captured during a night varies significantly from year to year. Uneven availability of observers, strongly varying local viewing conditions, and actual variation of TLE-producing potential of thunderstorms contribute to this variation. According to the experience, nevertheless, most sprites were captured in June while the greatest number of sprite halos have been detected from Baja so far in September.

Acknowledgements

This work was supported by the National Research, Development and Innovation Office, Hungary (NKFIH; grant No. K115836).

References

AllMetSat (2021). Retrieved November 30, 2021, from https://hu.allmetsat.com/kepek/sat24_europe_ir.php

Arnone, E., Bór, J., Chanrion, O. et al. (2020). Climatology of Transient Luminous Events and Lightning Observed Above Europe and the Mediterranean Sea. *Surveys in Geophysics, 41*, 167–199, https://doi.org/10.1007/s10712-019-09573-5

BlitzOrtung (2021). Retrieved November 30, 2021, from https://www.blitzortung.org

Bór, J., Sátori G., & Betz H.D. (2009). Observation of TLEs in Central Europe from Hungary Supported by LINET. *AIP Conference Proceedings, 1118*(73), https://doi.org/10.1063/1.3137716

Bór, J. (2013). Optically perceptible characteristics of sprites observed in Central Europe in 2007–2009. *Journal of Atmospheric and Solar-Terrestrial Physics, 92*, 151-177, https://doi.org/10.1016/j.jastp.2012.10.008

Bór, J., Zelkó, Z., Hegedüs, T., Jäger, Z., Mlynarczyk, J., Popek, M., & Betz, H. D. (2018). On the series of +CG lightning strokes in dancing sprite events. *Journal of Geophysical Research: Atmospheres, 123*, 11,030–11,047, https://doi.org/10.1029/2017JD028251

ESTOFEX (2021). Retrieved November 30, 2021, from https://www.estofex.org/

Gordillo-Vázquez, F.J., & Pérez-Invernón, F.J. (2021). A review of the impact of transient luminous events on the atmospheric chemistry: Past, present, and future. *Atmospheric Research, 252*, 105432, https://doi.org/10.1016/j.atmosres.2020.105432

Hegedüs, T., Szatmáry, K., & Vinkó, J. (1992). Light-curve and O-C Diagram Analysis of RZ Cassiopeiae. *Astrophysics and Space Science, 187*, 57-74., https://doi.org/10.1007/BF00642687

Hsu, R.-R., Su, H.-T., Chen, A. B.-C., & Kuo, C.-L. (2017). Selected results from the ISUAL/FORMOSAT2 mission. *Terrestrial, Atmospheric and Oceanic sciences journal, 28*, 525-544, https://doi.org/10.3319/TAO.2016.08.23.01

Ill, M. (1983). *Structure of the upper atmosphere as inferred from deceleration of satellites and on-board measurements* (translated from the Hungarian title: *A felsőlégkör szerkezete a műholdak fékeződése és fedélzeti mérések alapján)* [Doctoral dissertation, Hungarian Academy of Sciences] REAL-d. http://real-d.mtak.hu/1039/

Kotroni, V. & Lagouvardos, K. (2016). Lightning in the Mediterranean and its relation with sea-surface temperature. *Environmental Research Letters, 11*(3), 034006, https://doi.org/10.1088/1748-9326/11/3/034006

LightningMaps.org (2021). Retrieved November 30, 2021, from https://www.lightningmaps.org/

Meteologix (2021). Retrieved November 30, 2021, from https://meteologix.com/hu/lightning/europe

Mitnyan, T., Bódi, A., Szalai, T., Vinkó, J., Szatmáry, K., Borkovits, T., Bíró, B.I., Hegedüs, T., Vida, K., & Pál, A. (2018). The contact binary VW Cephei revisited: Surface activity and period variation. *Astronomy and Astrophysics, 612*, A91, 14 p., https://doi.org/10.1051/0004-6361/201731402

Neubert, T., Østgaard, N., Reglero, V. et al. (2019). The ASIM Mission on the International Space Station. *Space Science Reviews, 215*, 26, https://doi.org/10.1007/s11214-019-0592-z

Pasko, V.P., Yair, Y., & Kuo, C.L. (2012). Lightning Related Transient Luminous Events at High Altitude in the Earth's Atmosphere: Phenomenology, Mechanisms and Effects. *Space Science Reviews, 168*, 475–516, https://doi.org/10.1007/s11214-011-9813-9

Rakov, V.A. & Uman, M.A. (2007). *Lightning: Physics and Effects*. New York, USA: Cambridge University Press, ISBN 9781107268555

Saltikoff, E., Haase, G., Delobbe, L., Gaussiat, N., Martet, M., Idziorek, D., Leijnse, H., Novák, P., Lukach, M., & Stephan, K. (2019). OPERA the Radar Project. *Atmosphere, 10*(6), 320, https://doi.org/10.3390/atmos10060320

Siingh, D., Singh, R.P., Singh, A.K. et al. (2012). Discharges in the Stratosphere and Mesosphere. *Space Science Reviews, 169*, 73–121, https://doi.org/10.1007/s11214-012-9906-0

Singh, A.K., Siingh, D., Singh, R.P., & Mishra, S. (2011). Electrodynamical Coupling of Earth's Atmosphere and Ionosphere: An Overview. *International Journal of Geophysics, 2011*, 971302, https://doi.org/10.1155/2011/971302

Schmetz, J., Tjemkes, S.A., Gube, M., & van de Berg, L. (1997). Monitoring deep convection and convective overshooting with METEOSAT. *Advances in Space Research, 19*(3), 433-441, https://doi.org/10.1016/S0273-1177(97)00051-3

Soula, S., Defer, E., Füllekrug, M., van der Velde, O., Montanya, J., Bousquet, O., Mlynarczyk, J., Coquillat, S., Pinty, J.-P., Rison, W., et al. (2015). Time and space correlation between sprites and their parent lightning flashes for a thunderstorm observed during the HyMeX campaign. *Journal of Geophysical Research: Atmospheres, 120*, 11552– 11574, https://doi.org/10.1002/2015JD023894

Surkov V.V. & Hayakawa M. (2020). Progress in the Study of Transient Luminous and Atmospheric Events: A Review. *Surveys in Geophysics, 41*, 1101-1142, https://doi.org/10.1007/s10712-020-09597-2

van der Velde, O. A., Montanyà, J., Soula, S., Pineda, N., & Mlynarczyk, J. (2014). Bidirectional leader development in sprite-producing positive cloud-to-ground flashes: Origins and characteristics of positive and negative leaders. *Journal of Geophysical Research: Atmospheres, 119*, 12755–12779, https://doi.org/10.1002/2013JD021291

Vinkó, J., Sárneczky, K., Takáts, K., Marion, G.H., Hegedüs, T., Bíró, I.B., Borkovits, T., Szegedi-Elek, E., Farkas, A., Klagyivik, P., Kiss, L.L., Kovács, T., Pál, A., Szakáts, R., Szalai, N., Szalai, T., Szatmáry, K., Szing, A., Vida, K., & Wheeler, J.C. (2012). Testing supernovae Ia distance measurement methods with SN 2011fe. *Astronomy & Astrophysics, 546*, A12, https://doi.org/10.1051/0004-6361/201220043

Wang, Y., Lu, G., Ma, M., Zhang, H., Fan, Y., Liu, G., Wan, Z., Wang, Y., Peng, K-M, Peng, C., Liu, F., Zhu, B., Ni, B., Gu, X., Chen, L., Yi, J., & Zhou, R (2019). Triangulation of red sprites observed above a mesoscale convective system in North China. *Earth and Planetary Physics, 3*, 111-125, http://doi.org/10.26464/epp2019015